

Fractional quantum Hall states by Feynman’s diagrammatic expansion

Ben Currie and Evgeny Kozik

Department of Physics, King’s College London, Strand, London WC2R 2LS, United Kingdom

(Dated: December 31, 2024)

The fractional quantum Hall (FQH) effect arises from strong electron correlations in a quantising magnetic field, and features exotic emergent phenomena such as electron fractionalisation. Using the diagrammatic Monte Carlo approach with the combinatorial summation algorithm, we obtain results with controlled accuracy for the microscopic model of interacting electrons in the lowest Landau level. As the temperature is lowered, we study the development and emergence of the incompressible $1/3$ -filled FQH state. By analysing the long-time decay of the Green’s function, we find spectral properties consistent with an energy gap near $1/3$ -filling, while at half-filling an anomalous power law scaling is observed for short-range interaction screening, indicative of a non-Fermi liquid metal. Our work provides the first demonstration that fractionalised phases of matter can be reliably described with Feynman’s diagrammatic technique in terms of the fundamental electronic degrees of freedom, while also showing applicability of expansions in the bare Coulomb potential for precision calculations.

The application of a strong magnetic field to a two-dimensional electron gas leads to a rich variety of quantum phases. The resulting formation of perfectly flat bands – the well-known Landau levels – provides an ideal environment for electronic correlations at partial band filling, where Coulomb interactions dominate. This is perhaps evidenced best by the emergence of the fractional quantum Hall (FQH) states [1, 2], which are prototypical examples of topologically ordered phases of matter and which play host to low-energy excitations with fractional charge and statistics [3, 4]. While a remarkable amount of the Landau-level physics is described extremely well in terms of composite Fermions [5–10], including not only the FQH states but also the composite Fermi liquids at even denominator fillings, an understanding of the effect based solely on the electronic degrees of freedom has thus far not been achieved. Moreover, very little is known about the possible finite-temperature phases.

The lack of kinetic energy implies that the physics of partially filled Landau levels is inherently driven by strong electron correlations, which is challenging to study due to the absence of a small parameter. This has thus far prevented the development of controlled calculational schemes to study the microscopic electronic theory in the thermodynamic limit. Instead, controlled numerical solutions have come only from intrinsically finite-size methods such as exact diagonalisation [11–17] and DMRG [18–24]. Moreover, effective field theories based on composite Fermions provide qualitatively correct physics at mean-field level, but the systematic improvement by incorporating higher-order diagrams is hindered by the complexity of the perturbative expansion, which is an expansion in an emergent gauge field.

In this paper, we study the microscopic theory of electrons in the partially filled lowest Landau level (LLL) in terms of the bare electrons and include the effect of interactions order-by-order by an exact diagrammatic expansion around the non-interacting limit. Owing to the macroscopic degeneracy of the partially filled LLL, one might object that such a perturbation theory is not well-

defined, due to the complete restructuring of the state when arbitrarily weak interactions are turned on: a consequence of the fact that the interaction provides the only energy scale V . However, the introduction of a finite temperature T supplies an additional energy scale, and thereby also provides a perturbative regime in which $V/T \ll 1$. A qualitative change will occur as we pass from this regime to the strong coupling limit $V/T \gg 1$, in which the FQH states are expected to emerge via a smooth crossover. This is similar to the viewpoint exploited in controlled diagrammatic calculations for a state qualitatively distinct from the non-interacting limit, for example, in the metal-to-insulator crossover in the $2d$ Hubbard model [25, 26]. However, previous approximate diagrammatic approaches to the LLL in terms of the fundamental electronic degrees of freedom have not found a FQH state [27–30]. Other results in the thermodynamic limit based on a high-temperature expansion were restricted to temperatures much larger than the gap [31, 32]. A previous study by the present authors [30] based on an exact resummation of a specific subset of diagrams, corresponding to the self-consistent GW approximation, gave a non-Fermi liquid state in a broad range of filling fractions, but no evidence for FQH states was seen.

Here we represent the solution by a formally exact Feynman-diagrammatic expansion in the bare Coulomb potential with variable screening and evaluate the series numerically exactly using the diagrammatic Monte Carlo (DiagMC) technique [33–36] with the deterministic combinatorial summation (CoS) of all diagram integrands [37]. The flexibility of the CoS framework allows us to significantly improve the convergence properties of the series by compensating all diagrams that contain insertions contributing to the exact density with an appropriate shift of the chemical potential [35, 38]. Through calculating the expansion coefficients with high accuracy up to a sufficiently high diagram order ($n = 7$ in practice), we can control the precision of reconstructing the results from the series in regimes where it proves

divergent. We demonstrate the emergence of the FQH state at 1/3 filling of the LLL and probe its development as the temperature is lowered by studying the density against chemical potential (the equation of state): We observe a prominent plateau at 1/3 developing at low temperature, concomitant with compressibility saturating to a non-zero value at half-filling. Correspondingly, a gap opens in the single-electron spectral function $\rho(\omega)$ at 1/3-filling, while the spectral function of the 1/2 state depends strongly on the interaction range: for short-range interactions a non-Fermi liquid metal with $\rho(\omega) \propto \omega^{-0.56(2)}$ is found, while for long-range interactions a pseudo-gap emerges at a temperature consistent with experiments. Our results demonstrate that the emergence of an FQH state can be probed by a Feynman diagrammatic expansion method relying on an extrapolation of a large but ultimately finite number of diagram orders. It also proves that, despite their intrinsic divergence, expansions in the bare Coulomb potential are a viable approach to many-electron systems, which opens the door to more tractable simulations of real materials.

We study the continuum model of electrons in two dimensions subject to a uniform and perpendicular magnetic field with strength B and with density-density interactions. The corresponding Hamiltonian is

$$H = \sum_i \frac{1}{2m} (-i\partial_{\mathbf{r}_i} + \mathbf{A}(\mathbf{r}_i)) + \frac{\xi}{2} \sum_{i,j} V(\mathbf{r}_i - \mathbf{r}_j), \quad (1)$$

where \mathbf{A} is the vector potential corresponding to the external magnetic field, $V(\mathbf{r}_i - \mathbf{r}_j)$ is the Coulomb potential between the electrons at the $2d$ -vector coordinates $\mathbf{r}_{i,j}$ and ξ is an auxiliary expansion parameter, which can be viewed as a (dimensionless) coupling constant set to unity at the end of the calculation. In the non-interacting limit ($\xi = 0$), the single-particle spectrum reduces to the familiar Landau levels, which have a degeneracy per unit area $\mathcal{D} = 1/2\pi\ell_B^2$ and are spaced in energy by $\hbar\omega_B$, where $\omega_B = eB/m$ is the cyclotron frequency and $\ell_B = \sqrt{\hbar/eB}$ is the magnetic length. For simplicity, we consider the large- B limit with $\omega_B \gg e^2/\ell_B$, such that all electrons occupy the lowest Landau level, and all higher levels are projected out; generalisations are straightforward.

Our observable of interest is the fully interacting finite-temperature Matsubara Green's function projected onto the LLL, defined as [39]

$$G(\mathbf{r}_1\mathbf{r}_2, \tau) = -\langle \mathcal{T} \tilde{\phi}(\mathbf{r}_1, \tau) \tilde{\phi}^\dagger(\mathbf{r}_2, 0) \rangle, \quad (2)$$

where $\tilde{\phi}$ is the LLL-projected electron annihilation operator and \mathcal{T} is the time-ordering operator for the imaginary time τ . Remarkably, provided the translational symmetry is unbroken, the spatial dependence of G is independent of the interaction strength, and is given by

$$G(\mathbf{r}_1\mathbf{r}_2, \tau) = \frac{1}{2\pi\ell_B^2} G(\tau) e^{-\frac{1}{4\ell_B^2} |\mathbf{r}_1 - \mathbf{r}_2|^2} e^{i\varphi_{\mathbf{r}_1, \mathbf{r}_2}}, \quad (3)$$

where

$$\varphi_{\mathbf{r}_1, \mathbf{r}_2} = \frac{2\pi}{\phi_0} \int_{\mathbf{r}_1}^{\mathbf{r}_2} \mathbf{A}(\mathbf{x}) \cdot d\mathbf{x} \quad (4)$$

is the Aharonov-Bohm phase picked up by an electron traversing the path from \mathbf{r}_1 to \mathbf{r}_2 , and where $\phi_0 = h/e$ is the flux quantum. Here, $G(\tau)$ is the (gauge-invariant) Green's function in the basis of LLL states, whose precise form depends on the interaction strength and encodes the single-electron excitation properties of the system.

Diagrammatic expansions in the bare Coulomb potential are generally avoided due to two notorious issues: (i) the Dyson collapse argument [40] implies that such an expansion in continuous space has zero convergence radius and (ii) the long-range nature of the potential makes certain individual diagrams diverge upon integration over spatial coordinates. The zero convergence radius is a result of the discontinuous change of the state of the system, a collapse to infinite density, when the sign of the coupling constant ξ is flipped. Just as in lattice problems, it does not apply here because the density is bounded by the capacity of the (flat) LLL. The second problem is typically dealt with by screening the Coulomb interaction with dynamical polarisation and expanding in the screened coupling [41], which eliminates the divergent diagrams to avoid double counting. Another approach [42] is to introduce an auxiliary Yukawa screening, which renders the integrals convergent and can be tuned to accelerate the series convergence, and compensate the artificial screening by counter terms.

In contrast, we employ the Yukawa potential $V(r) = e^{-\lambda r}/r$ as the physical interaction and focus on the specific values $\lambda = 2\ell_B^{-1}$ and $\lambda = 0.5\ell_B^{-1}$ such that both the long-range Coulomb ($\lambda^{-1} > \ell_B$) and short-range ($\lambda^{-1} < \ell_B$) regimes are captured. The short-range regime is *a priori* a simpler case for observing FQH physics, is relevant in the context of model studies [13, 14, 43, 44], and naturally results in a better-behaved diagrammatic series. The regime of long-range interaction is of fundamental importance, both for the question of its effect on the possible FQH state and for studying the applicability of expansions in the Coulomb potential. In the pure Coulomb limit $\lambda \rightarrow 0$, all non-skeleton in the coupling channel diagrams—those that can be made disconnected by cutting any two interaction lines—diverge upon integration over internal variables. Thus, at small λ the series will be dominated by these terms, the role of which is to dress all interaction lines in all other diagrams by electron polarisation screening. A simple analysis (see Appendix A) shows that the divergence is due to a singularity at location $\xi_s \sim -\lambda$. Analytic continuation beyond the radius of convergence $|\xi_s|$ thus gives access to the Coulomb regime, in which the electron gas self-screens the long-range tail of the potential and thus all physical quantities are independent of λ (up to small corrections).

We compute $G(\tau)$ directly in the thermodynamic limit and at finite temperature T in the DiagMC framework [33–36]. In this approach, an arbitrary physical ob-

servable A is obtained—without approximations—from its Taylor series $A = \sum_{n=0}^N a_n \xi^n$ in the parameter ξ up to some maximal diagram order N , whereby a_n is represented as a sum over all diagrams with n interaction lines. Within each order n , all diagram integrands are summed deterministically by the CoS algorithm [37] and integrated over the positions of the interaction vertices in space-imaginary-time by stochastic sampling, which gives the exact value of a_n with a known statistical error bar. We use the version of the algorithm with symmetrisation over all vertex permutations, which takes $\mathcal{O}(n^3 3^n)$ floating point operations to sum all connected diagram topologies of order n for spinless fermions [37]. The extra computational cost compared to $\mathcal{O}(n^2 2^n)$ for the series with ordered vertices is compensated by the much smaller Monte Carlo variance for the symmetrised integrand.

To improve the convergence properties of the series [35, 38], we formulate the expansion in terms of the propagator partially dressed by the bold Hartree-Fock self-energy, as in the original DiagMC scheme [35]:

$$\tilde{G}_0(i\omega) = (i\omega + \mu - \Sigma_{\text{HF}}^{\text{bold}})^{-1}, \quad (5)$$

where μ is the chemical potential, $\Sigma_{\text{HF}}^{\text{bold}} = V_{\text{HF}}\nu$ with ν the exact filling fraction and $V_{\text{HF}} = (1/2\pi\ell_B^2) \times \int d^2\mathbf{r} V(\mathbf{r})(1 - e^{-\mathbf{r}^2/2\ell_B^2})$ is a constant equal to the uniform component of the Hartree-Fock effective potential. To avoid double-counting, all diagrams containing an insertion that is part of $\Sigma_{\text{HF}}^{\text{bold}}$ must be excluded in the determination of a_n . This is straightforward to implement within the CoS approach by forbidding such diagrams during the construction of the computational graph [37], the corresponding increase in the computational cost of evaluating which is insignificant for the expansion orders considered. In practice, the expansion in \tilde{G}_0 is implemented by fixing the shifted chemical potential $\tilde{\mu} = \mu - \Sigma_{\text{HF}}$ and reconstructing the physical potential μ when the exact ν is found.

We extrapolate the series to infinite diagram order using the Padé method [45], whereby a sequence of rational approximants are constructed based on the Taylor series coefficients alone, and are used to reconstruct the function at the physical coupling $\xi = 1$. The discrepancy between different approximants with arbitrary free parameters yields the total systematic error of the extrapolation, as explained in Ref. [46]. An example of such an extrapolation, together with the partial sum of the corresponding series is shown in Fig.1. This method also allows determination of the dominant singularities of the function behind the series. Since we find evidence for two pairs of singularities located at approximately equal radius for $\lambda = 2\ell_B^{-1}$, we restrict to approximants capable of capturing four or more singularities in this case, while three singularities are sufficient for $\lambda = 0.5\ell_B^{-1}$.

The dependence of the filling fraction ν , obtained from the Green's function via $\nu = -G(\beta^-)$, on the chemical potential is shown in Fig.2a for $\lambda = 2\ell_B^{-1}$ and for $\lambda = 0.5\ell_B^{-1}$ in Fig.2b. Due to the symmetry $\nu \rightarrow 1 - \nu$

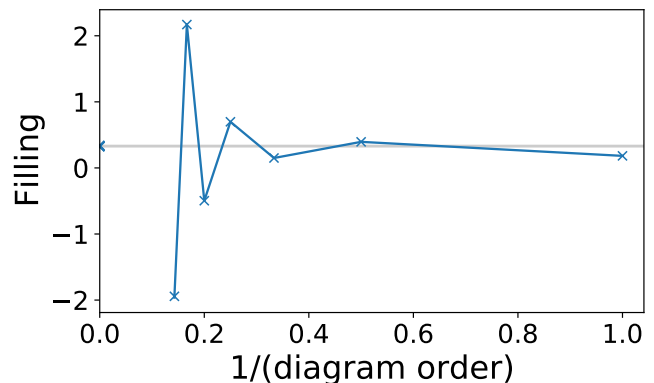


FIG. 1. Partial sum of the filling fraction against inverse diagram order up to order 7 for $\lambda = 0.5\ell_B^{-1}$, shifted chemical potential $\tilde{\mu} = -0.06e^2/\ell_B$ (defined in the main text), physical chemical potential $\mu = -0.29(1)e^2/\ell_B$ and temperature $T = 0.0621e^2/\ell_B$. The uncertainty in the extrapolated value is shown as the grey shaded region. The alternating divergence of the series is due to the Coulomb singularity on the negative real axis. The statistical error bars are smaller than the symbol size.

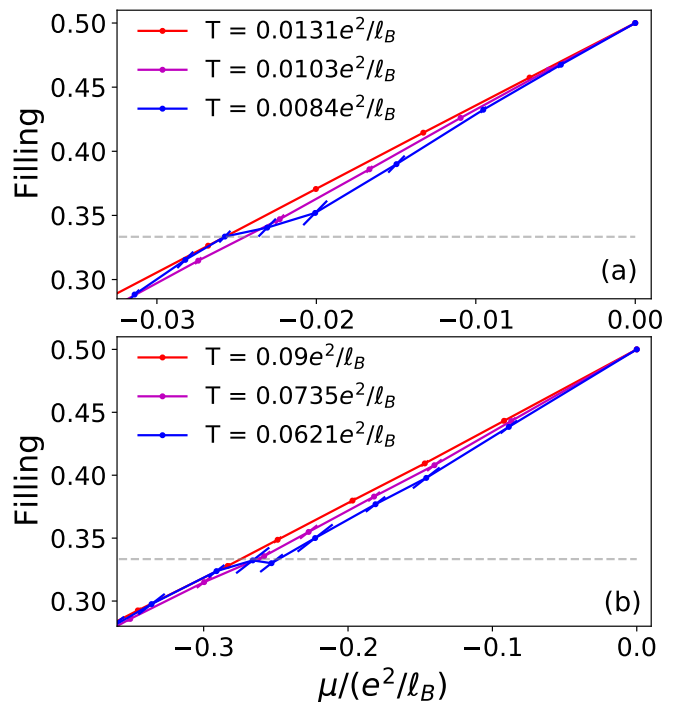


FIG. 2. The equation of state for the lowest Landau level model (1) with Yukawa potential (defined in the main text) and screening parameter $\lambda = 2\ell_B^{-1}$ (a) and $\lambda = 0.5\ell_B^{-1}$ (b) at different temperatures.

for $\mu \rightarrow -\mu$, only negative chemical potentials are shown. At high temperatures, where the series converges quickly, the equation of state is featureless, and the system is compressible for all fillings shown. However, as the temperature is lowered, a clear plateau is formed around the filling $\nu = 1/3$, indicative of the opening of a gap and the

formation of the $1/3$ FQH state. The size of the plateau provides a rough estimate for the gap size, which after accounting approximately for thermal broadening effects is consistent with the values $\Delta(\lambda = 2) \approx 0.01e^2/\ell_B$ and $\Delta(\lambda = 0.5) \approx 0.07e^2\ell_B$. The reduced gap in the larger screening λ case is due to the weakening of the interaction energy scale by the reduced potential range and is consistent with the similar rescaling of the corresponding T and μ . In the $\lambda \rightarrow \infty$ limit, this reduction is by the factor $1/\lambda^3$. Hence, for large $\lambda > \ell_B^{-1}$ we can account approximately for the reduction by multiplying all energy scales by λ^3 , which gives a gap size in qualitative agreement with previous numerical estimates for both λ values [47]. On the other hand, at half-filling, the system remains compressible down to the lowest temperatures, with an apparent saturation of the compressibility to the zero temperature regime.

Mathematically, the emergence of the plateau at $\nu = 1/3$ appears to be due to a particular structure of singularities in the Taylor series for density or Green's function. As $\tilde{\mu}$ is increased towards $\nu = 1/3$, the levelling of the curve coincides with a rapid movement of a complex-conjugate pair of apparent singularities with a large positive real part into the circle $|\xi| = 1$. A further increase of $\tilde{\mu}$ towards half-filling ($\tilde{\mu} = 0$) does not shift them significantly. However, a sequence of plateaus at odd denominator fractions is expected to emerge with further cooling (beyond that in Fig. 2), with the next one being at $\nu = 2/5$, since its gap is estimated at a half of that at $\nu = 1/3$ [47]. We can thus conjecture that the $\nu = 2/5$ state could be due an additional pair of singularities approaching $|\xi| = 1$ from the positive side of the real axis on top of the structure defined by the $1/3$ state in the range $1/3 < \nu \leq 1/2$, and to capture it reliably evaluation of the series to a higher order with similar error bars ($\lesssim 1\%$) would be required. This potential hierarchy in the singularity structure could resemble the hierarchy of the underlying charge fractionalisation [4, 13, 48].

A key diagnostic into the low-energy properties of the state is offered by the decay of the Green's function at long imaginary times. Provided the many-body state has reached its low-temperature limit, so that the temperature merely activates low-energy excitations, insulating states generally correspond to an exponential dependence on τ , while metallic states have power law dependence $\tau^{\gamma-1}$ ($\gamma = 0$ for a Landau Fermi liquid). In particular, it follows from the spectral representation that the electron spectral function $\rho(\omega)$ near $\omega = 0$ can be probed by examination of the quantity $\tilde{\rho} = -\beta G(\tau = \beta/2)$ [49]. The temperature dependence of this quantity is shown in Fig. 3. At the lowest temperatures, our data for $\nu = 1/3$ is consistent with the opening of a gap in $\rho(\omega)$ at a temperature at which the plateau emerges in the equation of state (Fig.2a). At half-filling ($\nu = 1/2$) and $\lambda = 2\ell_B^{-1}$, we see that $\tilde{\rho}(T)$ crosses over from the high-temperature behaviour $\tilde{\rho}(T) \propto 1/T$ to an anomalous scaling $\tilde{\rho}(T) \propto T^{-\gamma}$ with $\gamma = 0.56(2)$ at low temperatures, resulting from a long-time decay of the Green's function $G(\tau) \propto \tau^{\gamma-1}$.

Such a scaling is consistent with a spectral function that depends on frequency as $\rho(\omega) \propto \omega^{-\gamma}$. A similar strange-metal scaling, with an exponent $1/4 < \gamma < 1$ that depends on the interaction range λ , was suggested previously based on the self-consistent GW approximation [30]. This was found to give for the Coulomb potential ($\lambda = 0$) an exponent $\gamma \rightarrow 1/2$ in the zero temperature limit, while for the Trugman-Kivelson potential [43], which is obtained in the limit $\lambda \rightarrow \infty$, one finds $\gamma = 1/4$. The actual temperature scale for the crossover to the strange metal regime is about an order of magnitude lower than that observed in the study of Ref. [30] for the same Yukawa parameter, which implies that the GW approximation, despite the self-consistent renormalisation of the Green's function and Coulomb interaction, still misses important fluctuations. This anomalous scaling sets in only for the short-range potential $\lambda = 2\ell_B^{-1}$ in our study: Fig. 3 shows that, for $\lambda = 0.5\ell_B^{-1}$, an apparent suppression (pseudo-gap) in the spectral function develops gradually over a very broad temperature range without a clear power-law regime.

The electron spectral function has been probed experimentally by measurements of the tunnelling current between two parallel $2d$ electron gas systems in a large magnetic field [50–55]. They observe a strong suppression in the current in a wide range of the LLL fillings (including $\nu = 1/2$ and $\nu = 1/3$) at low temperatures, suggesting an exponential low-frequency dependence of the form $\rho(\omega \rightarrow 0) = e^{-\omega_0/\omega}$, where ω_0 is a roughly filling independent energy scale on the order of $0.5e^2/\ell_B$. This pseudo-gap behaviour is seen at $T = 0.66$ K, while at magnetic fields corresponding to half-filling the gap is almost completely filled in at $T = 9.5$ K [52]. At half-filling, for $\lambda = 2\ell_B^{-1}$ and at magnetic field $B = 13$ T, these temperatures correspond to $0.0004e^2/\ell_B$ and $0.006e^2\ell_B$ in our units, respectively, which are both lower than the temperatures we reach in Fig.3. On the other hand, for $\lambda = 0.5\ell_B^{-1}$, a suppression of the spectral function is observed at $T \approx 0.05e^2/\ell_B$ corresponding to $T \approx 10$ K. The striking difference between the half-filling behaviour for the two Yukawa parameters highlights the importance of the potential range in determining the low-energy spectral properties.

In summary, we have studied the minimal microscopic model of FQH physics and demonstrated that the development of the $1/3$ -filled Laughlin state can be obtained with controlled accuracy via the standard diagrammatic expansion around the non-interacting limit at finite temperatures. A low-temperature plateau in the equation of state emerges at $1/3$ -filling due to a particular analytic structure of the resulting Taylor series and despite the absence of any prior information about it in the microscopic model or the construction of the diagrammatic expansion. This is fundamentally different to the DiagMC solution for the insulating regime of the $2d$ Hubbard model [25, 26], where the opening of the gap at half-filling is predetermined by the particle-hole symmetry and the ensuing nesting of the Fermi surface. In con-

trast, for short range interactions the half-filled LLL is a non-Fermi liquid metal consistent with that proposed recently by an approximate self-consistent *GW* theory [30], while for longer range interactions a broad crossover to a pseudogapped regime is observed which is consistent with experiments [52]. This is also highly non-trivial because the low-order solution for $\nu = 1/2$ is actually insulating at a relatively high temperature $T \approx 0.1e^2/\ell_B$, and both the low temperature anomalous metallic and pseudo-gapped properties are only recovered at higher orders.

Our work provides a new window for studying the emergence of topologically non-trivial phases as a function of temperature, and is the first demonstration that a phase of matter featuring fractionalisation can be obtained in a diagrammatic expansion in terms of the prime electronic degrees of freedom. While we have focussed only on the lowest Landau level here, the approach can be readily applied to include any number of Landau levels and could provide a novel probe for higher-filling states, such as those thought to possess non-Abelian anyonic excitations [56] and are promising as potential platforms for fault-tolerant topological quantum computation [57].

More generally, this shows that systems with completely flat bands can be reliably studied by finite-temperature diagrammatic expansions in the bare coupling, which *a priori* may seem counter-intuitive because the absence of kinetic energy appears to make a perturbation theory impossible. In fact, since the temperature is the only energy scale for the interaction, the expansion in the powers of ξ is equivalent to expanding in V/T about $V/T = 0$, which is a well-defined starting point. Provided the low-temperature state is not separated from this starting point by a phase transition, it is natural for a Taylor series in $\xi V/T$ to be able to capture its properties with enough expansion coefficients at hand. An advantage of the diagrammatic formulation of such a high-temperature expansion is that there are many established tools for accelerating it [58], as we do here by a particular shift of the chemical potential.

One of the main difficulties in simulating real materials in the diagrammatic framework [41, 59] is the derivation and parametrisation of the dynamically screened interaction W [60]. The Coulomb interaction V , in contrast, is static and straightforward to obtain in any basis. Our results suggest that diagrammatic expansions in V with a regularisation of the integrals by $\lambda \rightarrow 0$ can be used for controlled calculations when the number of computed expansion coefficients is sufficient for a reliable resummation of the series beyond the convergence radius $\sim |\lambda|$. Since the limiting singularity is of a very simple general form (see Appendix A), the analytic continuation is robust already with a few diagram orders, which makes expansions in the bare Coulomb potential evaluated by DiagMC a promising route to controlled simulations of materials.

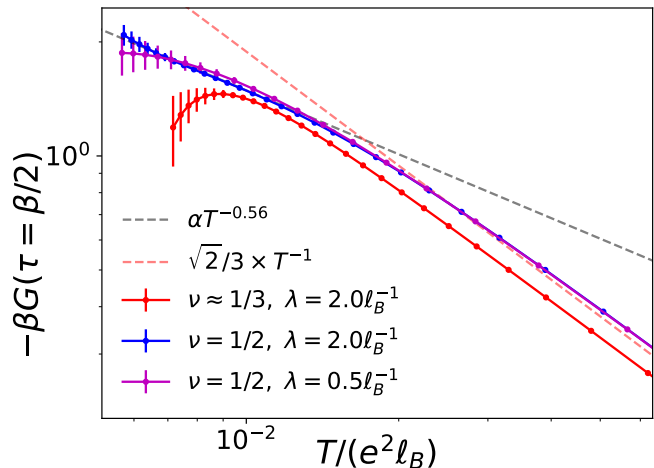


FIG. 3. The Green's function at the imaginary time $\tau = \beta/2$ —which serves as a proxy for the single-electron spectral function after multiplication by β —against temperature for the two values of the screening λ . Curves are at constant Hartree-Fock-shifted chemical potential $\tilde{\mu}$, which at half-filling corresponds to constant physical chemical potential $\tilde{\mu} = \mu = 0$ (blue and purple curves). The curve labelled $\nu \approx 1/3$ has a filling that varies from $\nu(T \rightarrow \infty) = 0.22$ to $\nu(T \rightarrow 0) = 1/3$. The temperatures for the data at $\lambda = 0.5\ell_B^{-1}$ have been divided by a factor of 8 for ease of comparison to the $\lambda = 2\ell_B^{-1}$ data. The high temperature asymptote, $\lim_{T \rightarrow \infty} G(\beta/2) = -\sqrt{\nu(1-\nu)}$, corresponding to $\nu = 1/3$ is shown as the red dashed curve. For all curves, the crossover from the high-temperature region, in which the Green's function remains close to its asymptote, to the low-temperature regime is seen to occur at the temperature scales $T \approx 0.01e^2/\ell_B$ for $\lambda = 2\ell_B^{-1}$ and $T \approx 0.06e^2/\ell_B$ for $\lambda = 0.5\ell_B^{-1}$, consistent with the temperature scales at which the plateaus emerge in Fig2.

ACKNOWLEDGMENTS

This work was supported by EPSRC through Grant No. EP/X01245X/1. The calculations were performed using King's Computational Research, Engineering and Technology Environment (CREATE).

Appendix A: Regularisation of the bare series by Yukawa screening

Within the bare series, all diagrams with insertions of the electron polarisation Π in any of the interaction lines are divergent for the pure Coulomb potential ($\lambda = 0$) due to integration of the internal vertices over space (or momentum). Let us regularise the integrals by $\lambda > 0$ and ask: given the divergence of these diagrams at $\lambda = 0$, how can we understand the limit $\lambda \rightarrow 0$ from the bare series? Consider, for example, the n -th order contribution to the screened interaction W , which will be dominated by the diagram containing the maximal number $(n - 1)$ of polarisation bubbles Π_0 . In the basis of LLL states, this diagram is (in units with $\ell_B = 1$; see Ref.[30] for details)

$$W_n(i\nu) = \int_0^\infty d\rho \rho \xi U(\rho) (\xi \Pi_0(i\nu) U(\rho))^{n-1}, \quad (\text{A1})$$

where $\Pi_0(\tau) = G(\tau)G(-\tau)$ is the bare electron polarisation, $G(\tau)$ is the Green's function in the LLL basis defined in Eq.3, $U(\rho) = e^{-\frac{1}{2}\rho^2} / \sqrt{\rho^2 + \lambda^2}$ is the Yukawa-screened Coulomb potential in this basis and in momentum space, and $i\nu$ is a bosonic Matsubara frequency. For $n = 2$ this diagram diverges as $\log \lambda$, and for $n > 2$ as λ^{2-n} , in the $\lambda \rightarrow 0$ limit. In the former case, performing the integration over momentum yields

$$\begin{aligned} W_2(i\nu) &= \Pi_0(i\nu) \int_0^\infty d\rho \rho \left(\frac{\xi}{\sqrt{\rho^2 + \lambda^2}} e^{-\frac{1}{2}\rho^2} \right)^2 \\ &= -\xi^2 \Pi_0(i\nu) [\gamma/2 + \log(\lambda)] + \mathcal{O}(\lambda^2), \end{aligned} \quad (\text{A2})$$

where γ is the Euler-Mascheroni constant. For $n > 2$, due to the domination of the small- ρ region at $\lambda \rightarrow 0$, we can ignore the Gaussian factor, which yields

$$\begin{aligned} W_{n>2}(i\nu) &= \xi^n \Pi_0(i\nu)^{n-1} \int_0^\infty d\rho \rho \left(\frac{1}{\sqrt{\rho^2 + \lambda^2}} \right)^n \\ &= \frac{1}{n-2} \lambda^{-(n-2)} \xi^n \Pi_0^{n-1}(i\nu). \end{aligned} \quad (\text{A3})$$

For the sum of all such diagrams $W'(i\nu) = \sum_{n=2}^\infty W_n(i\nu)$, we thus obtain

$$\begin{aligned} W'(i\nu) &= W_2(i\nu) + \xi^2 \Pi_0(i\nu) \sum_{n=3}^\infty \frac{1}{n-2} [\lambda/\xi \Pi_0(i\nu)]^{-(n-2)} \\ &= \xi^2 \Pi_0(i\nu) [-\gamma/2 - \log(\lambda - \xi \Pi_0(i\nu)) + \mathcal{O}(\lambda^2)]. \end{aligned} \quad (\text{A4})$$

Since $\Pi_0 < 0$ we find a logarithmic singularity on the negative real axis at location $\xi_s = -\lambda/|\Pi_0|$. The bare series diverges at the physical coupling $\xi = 1$ when the natural screening length $\propto \Pi_0^{-1}$ is comparable to the artificial screening length λ^{-1} . However a resummation of the series for the log function beyond the convergence radius $|\xi_s|$ is straightforward and provides access to the Coulomb regime in which $\Pi^{-1} \ll \lambda^{-1}$, with a weak residual dependence on $\lambda \ll 1$.

While the calculation above focussed on the 2D electron gas in a strong magnetic field, a similar analysis was found to hold for the 3D electron gas in zero external field. In this case, the same calculation yields a square-root singularity located at $\xi_s = -\lambda^2/|\Pi|$. Therefore analytic continuation beyond the singularity at finite λ provides a general method for accessing Coulomb physics by a Feynman expansion in the bare potential, combined with an extrapolation to $\lambda = 0$.

-
- [1] D. C. Tsui, H. L. Stormer, and A. C. Gossard, Two-dimensional magnetotransport in the extreme quantum limit, *Phys. Rev. Lett.* **48**, 1559 (1982).
 - [2] H. L. Stormer, A. Chang, D. C. Tsui, J. C. M. Hwang, A. C. Gossard, and W. Wiegmann, Fractional quantization of the Hall effect, *Phys. Rev. Lett.* **50**, 1953 (1983).
 - [3] D. Arovas, J. R. Schrieffer, and F. Wilczek, Fractional statistics and the quantum Hall effect, *Phys. Rev. Lett.* **53**, 722 (1984).
 - [4] B. I. Halperin, Statistics of quasiparticles and the hierarchy of fractional quantized Hall states, *Phys. Rev. Lett.* **52**, 1583 (1984).
 - [5] J. K. Jain, Composite-fermion approach for the fractional quantum Hall effect, *Phys. Rev. Lett.* **63**, 199 (1989).
 - [6] J. K. Jain, Theory of the fractional quantum Hall effect, *Phys. Rev. B* **41**, 7653 (1990).
 - [7] A. Lopez and E. Fradkin, Fractional quantum Hall effect and Chern-Simons gauge theories, *Phys. Rev. B* **44**, 5246 (1991).
 - [8] S. C. Zhang, T. H. Hansson, and S. Kivelson, Effective-field-theory model for the fractional quantum Hall effect, *Phys. Rev. Lett.* **62**, 82 (1989).
 - [9] B. I. Halperin, P. A. Lee, and N. Read, Theory of the half-filled Landau level, *Phys. Rev. B* **47**, 7312 (1993).
 - [10] R. Shankar and G. Murthy, Towards a field theory of fractional quantum Hall states, *Phys. Rev. Lett.* **79**, 4437 (1997).
 - [11] D. Yoshioka, B. I. Halperin, and P. A. Lee, Ground state of two-dimensional electrons in strong magnetic fields and $\frac{1}{3}$ quantized Hall effect, *Phys. Rev. Lett.* **50**, 1219 (1983).
 - [12] R. B. Laughlin, Quantized motion of three two-dimensional electrons in a strong magnetic field, *Phys. Rev. B* **27**, 3383 (1983).
 - [13] F. D. M. Haldane, Fractional quantization of the Hall effect: A hierarchy of incompressible quantum fluid states, *Phys. Rev. Lett.* **51**, 605 (1983).
 - [14] F. D. M. Haldane and E. H. Rezayi, Finite-size studies

- of the incompressible state of the fractionally quantized Hall effect and its excitations, *Phys. Rev. Lett.* **54**, 237 (1985).
- [15] G. Fano, F. Ortolani, and E. Colombo, Configuration-interaction calculations on the fractional quantum Hall effect, *Phys. Rev. B* **34**, 2670 (1986).
- [16] N. d'Ambrumenil and R. Morf, Hierarchical classification of fractional quantum Hall states, *Phys. Rev. B* **40**, 6108 (1989).
- [17] R. H. Morf, N. d'Ambrumenil, and S. Das Sarma, Excitation gaps in fractional quantum Hall states: An exact diagonalization study, *Phys. Rev. B* **66**, 075408 (2002).
- [18] N. Shibata and D. Yoshioka, Ground-state phase diagram of 2d electrons in a high Landau level: A density-matrix renormalization group study, *Phys. Rev. Lett.* **86**, 5755 (2001).
- [19] A. E. Feiguin, E. Rezayi, C. Nayak, and S. Das Sarma, Density matrix renormalization group study of incompressible fractional quantum Hall states, *Phys. Rev. Lett.* **100**, 166803 (2008).
- [20] D. L. Kovrizhin, Density matrix renormalization group for bosonic quantum Hall effect, *Phys. Rev. B* **81**, 125130 (2010).
- [21] M. P. Zaletel and R. S. K. Mong, Exact matrix product states for quantum Hall wave functions, *Phys. Rev. B* **86**, 245305 (2012).
- [22] Z.-X. Hu, Z. Papić, S. Johri, R. Bhatt, and P. Schmitteckert, Comparison of the density-matrix renormalization group method applied to fractional quantum Hall systems in different geometries, *Physics Letters A* **376**, 2157 (2012).
- [23] B. Estienne, Z. Papić, N. Regnault, and B. A. Bernevig, Matrix product states for trial quantum Hall states, *Phys. Rev. B* **87**, 161112 (2013).
- [24] M. P. Zaletel, R. S. K. Mong, and F. Pollmann, Topological characterization of fractional quantum Hall ground states from microscopic Hamiltonians, *Phys. Rev. Lett.* **110**, 236801 (2013).
- [25] F. Šimkovic, J. P. F. LeBlanc, A. J. Kim, Y. Deng, N. V. Prokof'ev, B. V. Svistunov, and E. Kozik, Extended crossover from a Fermi liquid to a quasiantiferromagnet in the half-filled 2d Hubbard model, *Phys. Rev. Lett.* **124**, 017003 (2020).
- [26] A. J. Kim, F. Šimkovic, and E. Kozik, Spin and charge correlations across the metal-to-insulator crossover in the half-filled 2d Hubbard model, *Phys. Rev. Lett.* **124**, 117602 (2020).
- [27] R. Tao and D. J. Thouless, Fractional quantization of Hall conductance, *Phys. Rev. B* **28**, 1142 (1983).
- [28] D. J. Thouless, Long-range order and the fractional quantum Hall effect, *Phys. Rev. B* **31**, 8305 (1985).
- [29] R. Haussmann, Electronic spectral function for a two-dimensional electron system in the fractional quantum Hall regime, *Phys. Rev. B* **53**, 7357 (1996).
- [30] B. Currie and E. Kozik, Strange metal to insulator transitions in the lowest Landau level, *Phys. Rev. Res.* **6**, 023210 (2024).
- [31] L. Zheng and A. MacDonald, High temperature perturbation study of two-dimensional interacting electrons in a partly-filled Landau level, *Surface Science* **305**, 101 (1994).
- [32] S. Sawatdiaree and W. Apel, On the high-temperature expansion for a partially filled lowest Landau level, *Physica E: Low-dimensional Systems and Nanostructures* **6**, 75 (2000).
- [33] N. V. Prokof'ev and B. V. Svistunov, Polaron Problem by Diagrammatic Quantum Monte Carlo, *Phys. Rev. Lett.* **81**, 2514 (1998).
- [34] N. Prokof'ev and B. Svistunov, Bold Diagrammatic Monte Carlo Technique: When the Sign Problem Is Welcome, *Phys. Rev. Lett.* **99**, 250201 (2007).
- [35] K. Van Houcke, E. Kozik, N. Prokof'ev, and B. Svistunov, Diagrammatic Monte Carlo, *Phys. Procedia* **6**, 95 (2010).
- [36] E. Kozik, K. Van Houcke, E. Gull, L. Pollet, N. Prokof'ev, B. Svistunov, and M. Troyer, Diagrammatic Monte Carlo for correlated fermions, *Europhys. Lett.* **90**, 10004 (2010).
- [37] E. Kozik, Combinatorial summation of Feynman diagrams, *Nature Communications* **15**, 7916 (2024).
- [38] W. Wu, M. Ferrero, A. Georges, and E. Kozik, Controlling Feynman diagrammatic expansions: Physical nature of the pseudogap in the two-dimensional Hubbard model, *Phys. Rev. B* **96**, 041105(R) (2017).
- [39] A. Abrikosov, L. Gorkov, I. Dzyaloshinski, and R. Silverman, *Methods of Quantum Field Theory in Statistical Physics*, Dover Books on Physics (Dover Publications, New York, 2012).
- [40] F. J. Dyson, Divergence of Perturbation Theory in Quantum Electrodynamics, *Phys. Rev.* **85**, 631 (1952).
- [41] L. Hedin, New method for calculating the one-particle green's function with application to the electron-gas problem, *Phys. Rev.* **139**, A796 (1965).
- [42] K. Chen and K. Haule, A combined variational and diagrammatic quantum Monte Carlo approach to the many-electron problem, *Nat. Commun.* **10**, 3725 (2019).
- [43] S. A. Trugman and S. Kivelson, Exact results for the fractional quantum Hall effect with general interactions, *Phys. Rev. B* **31**, 5280 (1985).
- [44] V. L. Pokrovsky and A. L. Talapov, A simple model for fractional Hall effect, *Journal of Physics C: Solid State Physics* **18**, L691 (1985).
- [45] G. A. Baker, Application of the Padé approximant method to the investigation of some magnetic properties of the Ising model, *Phys. Rev.* **124**, 768 (1961).
- [46] F. Šimkovic and E. Kozik, Determinant Monte Carlo for irreducible Feynman diagrams in the strongly correlated regime, *Phys. Rev. B* **100**, 121102(R) (2019).
- [47] J. K. Jain and R. K. Kamilla, Quantitative study of large composite-fermion systems, *Phys. Rev. B* **55**, R4895 (1997).
- [48] B. I. Halperin, Theory of the quantized Hall conductance, *Helv. Phys. Acta* **56**, 75 (1983).
- [49] W. O. Wang, J. K. Ding, B. Moritz, E. W. Huang, and T. P. Devereaux, DC Hall coefficient of the strongly correlated Hubbard model, *npj Quantum Materials* **5**, 51 (2020).
- [50] R. C. Ashoori, J. A. Lebens, N. P. Bigelow, and R. H. Silsbee, Equilibrium tunneling from the two-dimensional electron gas in GaAs: Evidence for a magnetic-field-induced energy gap, *Phys. Rev. Lett.* **64**, 681 (1990).
- [51] R. C. Ashoori, J. A. Lebens, N. P. Bigelow, and R. H. Silsbee, Energy gaps of the two-dimensional electron gas explored with equilibrium tunneling spectroscopy, *Phys. Rev. B* **48**, 4616 (1993).
- [52] J. P. Eisenstein, L. N. Pfeiffer, and K. W. West, Coulomb barrier to tunneling between parallel two-dimensional electron systems, *Phys. Rev. Lett.* **69**, 3804 (1992).

- [53] K. M. Brown, N. Turner, J. T. Nicholls, E. H. Linfield, M. Pepper, D. A. Ritchie, and G. A. C. Jones, Tunneling between two-dimensional electron gases in a strong magnetic field, *Phys. Rev. B* **50**, 15465 (1994).
- [54] J. P. Eisenstein, L. N. Pfeiffer, and K. W. West, Evidence for an interlayer exciton in tunneling between two-dimensional electron systems, *Phys. Rev. Lett.* **74**, 1419 (1995).
- [55] J. P. Eisenstein, T. Khaire, D. Nandi, A. D. K. Finck, L. N. Pfeiffer, and K. W. West, Spin and the Coulomb gap in the half-filled lowest Landau level, *Phys. Rev. B* **94**, 125409 (2016).
- [56] R. L. Willett, C. Nayak, K. Shtengel, L. N. Pfeiffer, and K. W. West, Magnetic-field-tuned Aharonov-Bohm oscillations and evidence for non-abelian anyons at $\nu = 5/2$, *PRL* **111**, 186401 (2013).
- [57] C. Nayak, S. H. Simon, A. Stern, M. Freedman, and S. Das Sarma, Non-abelian anyons and topological quantum computation, *Rev. Mod. Phys.* **80**, 1083 (2008).
- [58] A. J. Kim, N. V. Prokof'ev, B. V. Svistunov, and E. Kozik, Homotopic action: A pathway to convergent diagrammatic theories, *Phys. Rev. Lett.* **126**, 257001 (2021).
- [59] F. Aryasetiawan and O. Gunnarsson, The *GW* method, *Reports on Progress in Physics* **61**, 237 (1998).
- [60] D. A. Leon, C. Cardoso, T. Chiarotti, D. Varsano, E. Molinari, and A. Ferretti, Frequency dependence in *GW* made simple using a multipole approximation, *Phys. Rev. B* **104**, 115157 (2021).